Active storage of liquid hydrogen

Alberto Posada, Vasilios Manousiouthakis
Chemical & Biomolecular Engineering Department, University of California, Los Angeles, CA 90095, USA

Abstract

The use of a conduction-cooled, refrigerated and insulated storage vessel for liquid hydrogen is proposed as an alternative that can allow a reduction in the thickness of the vessel's insulation and can extend storage times by directing the in-leak heat towards one or few refrigerated cold sectors in the insulation of the vessel. This heat is conducted through one or few copper layers incorporated in the insulation. Although evaporative loss of hydrogen is prevented with the proposed design, refrigeration work must be provided to remove the in-leak heat. Allowing evaporation to produce hydrogen gas that can be used for power generation in the vehicle's fuel cell helps reduce the cooling load of the refrigerator.

Keywords: LH_2; hydrogen; conduction-cooling; thermal insulation; storage vessel; copper; fuel cell vehicle.

1. Introduction

The design of an effective on-board hydrogen storage system offers a challenging opportunity for engineers due to the low density of hydrogen at standard conditions (25 °C, 1 atm). Currently available technologies include storage of hydrogen as compressed gas, cryogenic liquid and metal hydride (adsorbed hydrogen) and have been compared by Aceves and coworkers [1,2], and James et al [3]. One avenue leading to high hydrogen densities is the use of liquid hydrogen either at atmospheric or even high pressures. The critical temperature of hydrogen however is T_c = 33.2 K, and thus liquid hydrogen storage requires a well-insulated storage vessel, with a significant fraction of the total vessel volume occupied by insulation. When storage space and/or time are design considerations, as is the case for long-term fuel storage on vehicles, alternatives are sought that make the most effective use of the available volume. In this work, we propose the use of a conduction-cooled, refrigerated and insulated storage vessel for liquid hydrogen, as an alternative that can allow a reduction in the thickness of the vessel's insulation and can extend storage times by directing the in-leak heat towards one or few refrigerated cold sectors in the insulation of the vessel. This heat is conducted through one or few copper layers incorporated in the insulation. A detailed description of this cooling effect, as applied to superconducting cables, has been presented in our previous work [4]. Directing the heat towards the cold sector(s) in the insulation of the vessel maintains the hydrogen in a liquid state, thus preventing evaporative losses, albeit at the cost of running the refrigerator(s). Allowing hydrogen evaporation to produce hydrogen gas that can be used for power generation in the vehicle's fuel cell can help reduce the cooling load of the refrigerator(s).

A basic design for a conduction-cooled liquid hydrogen storage vessel is proposed and a detailed numerical simulation of heat transfer in such a vessel is carried out using the software FEMLAB® version 2.3b. The remainder of the paper is organized as follows: in section 2 the proposed vessel design is described. The data used for the thermal conductivity of materials are presented in section 3. The governing set of partial differential equations that describe the temperature profile in the vessel is developed in section 4. In section 5, the numerical solution of the aforementioned differential equations is presented for the proposed vessel design and these results are discussed in section 6. Section 7 includes a brief comparison with active cooling of a cryogenic compressed hydrogen gas storage vessel, and conclusions are drawn in section 8.

2. Description of the system

A schematic of a conduction-cooled, spherical vessel, for the storage of liquid hydrogen, is presented in Fig 1a. The vessel's interior is an actively-cooled shield made of copper. The vessel wall is made of aluminum or a composite material with sufficient thickness to maintain a given pressure inside the vessel; it is surrounded by a layer of thermal insulator, another layer of copper and another layer of thermal insulator. Basic dimensions are shown in Fig. 1b. The insulated vessel is represented by a sphere with radius R. The space available for hydrogen storage is within the sphere with radius r_1 and is delimited by the copper shield. Adjacent, with external radius r_3, is the vessel wall. The outer copper layer, also represented by a hollow sphere, has internal radius r_4 and external radius r_5 (in white, see Fig. 1b). The two remaining hollow spherical annuli, filled with gray color and separated by the outer copper layer, represent the two layers of thermal insulation. The inner cold sector in the vessel, located in the region between $\theta = \theta_n$ and $\theta = \pi$, and between $r = r_1$ and $r = r_2$, is kept at 21 K through the use of a cryogenic refrigeration system, and the outer cold sector, located between $r = r_4$ and $r = r_5$, is kept at 80 K, also through refrigeration, while the ambient temperature is 300 K. The copper layers channel the heat that enters the vessel radially through the outer insulation layer in the θ-direction, towards the cold sectors, instead of allowing it to move in the radial direction towards the liquid hydrogen stored in the vessel.

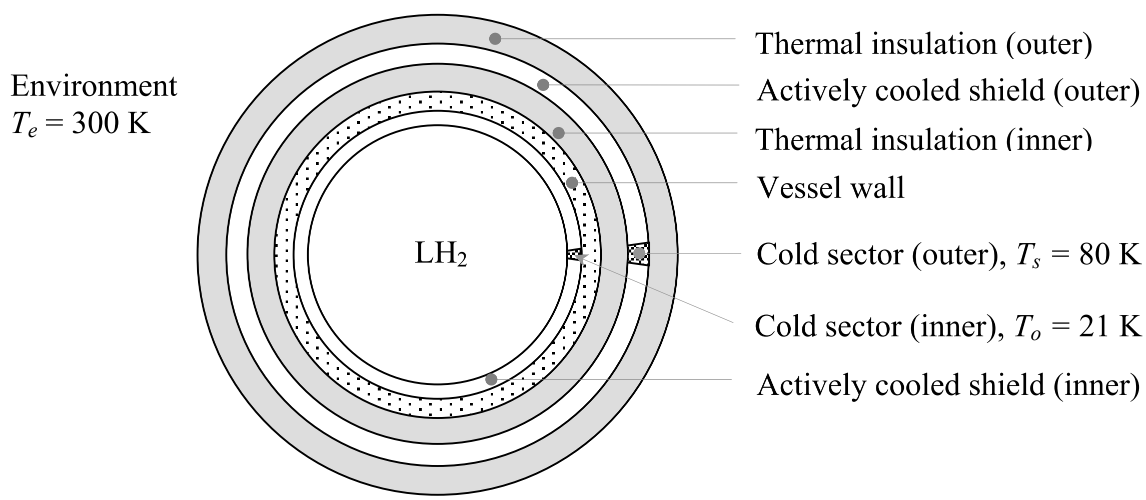

Fig 1a. Schematic of insulated liquid hydrogen storage spherical vessel.

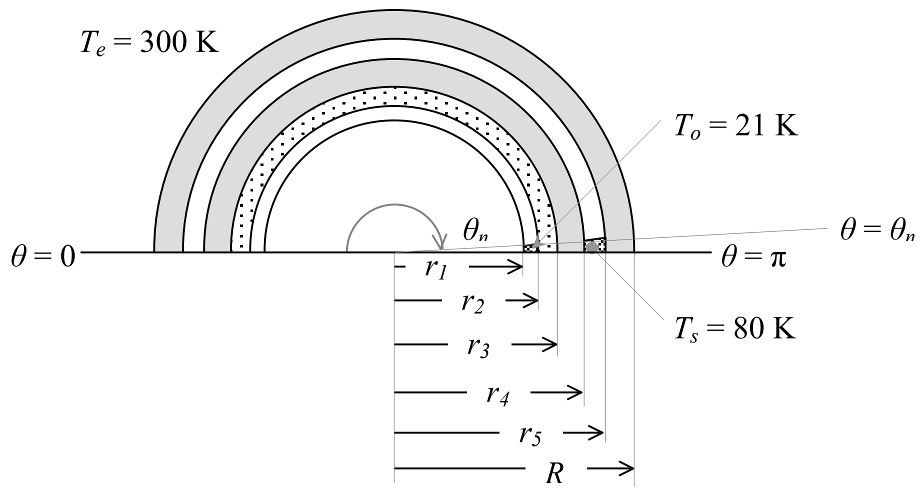

Fig 1b. Domain for heat transfer simulation. Plane *r-θ* of the spherical vessel for any fixed ϕ (ϕ rotation-axis is perpendicular to *θ* rotation-axis and parallel to the straight line that goes through *θ* = 0 and *θ* = π).

3. Thermal conductivity of materials

3.1. Copper

Equation (1) gives the thermal conductivity k_c (W/m-K) for an average sample of oxygen-free copper, as a function of temperature, *T* (K), [5].

$$\log k_c = \frac{2.2154 - 0.88068 \cdot T^{0.5} + 0.29505 \cdot T - 0.048310 \cdot T^{1.5} + 0.003207 \cdot T^2}{1 - 0.47461 \cdot T^{0.5} + 0.13871 \cdot T - 0.020430 \cdot T^{1.5} + 0.001281 \cdot T^2} \tag{1}$$

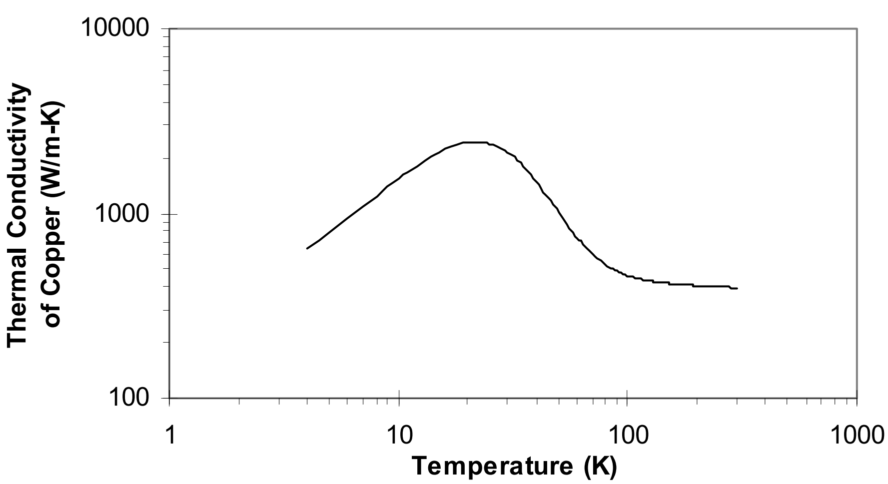

Fig 2. Thermal conductivity of copper, k_c, as calculated from equation (1).

The thermal conductivity for this material can vary widely depending upon the residual resistivity ratio, RRR. The values calculated with equation (1), and plotted in Fig. 2, are similar to those obtained using the model given by Simon et al., [6], for RRR=100. It can be noted from Fig. 2, that the thermal conductivity of copper at cryogenic temperatures reaches high values (over 2000 W/m-K).

3.2. Thermal insulator

A multilayer insulation is considered. It consists of alternating layers of a highly reflecting material, and a low-conductivity spacer. The value of the insulation's thermal conductivity used in this work, $k_m = 1 \times 10^{-4}$ W/m-K, is the same as that used by Aceves et al. [1].

3.3. Vessel wall

Aluminum was considered to be the metal comprising the vessel wall. Equation (2) gives the thermal conductivity k_w (W/m-K) for 6061-T6 aluminum, as a function of temperature, T (K), [5].

$$\begin{aligned}\log k_w &= 0.07918 + 1.0957 \cdot \log T - 0.07277 \cdot (\log T)^2 + 0.08084 \cdot (\log T)^3 \\ &+ 0.02803 \cdot (\log T)^4 - 0.09464 \cdot (\log T)^5 + 0.04179 \cdot (\log T)^6 - 0.00571 \cdot (\log T)^7\end{aligned} \quad (2)$$

3.4. Hydrogen

The thermal conductivity of liquid hydrogen has been considered to be constant and equal to k_h = 0.10434 W/m-K, corresponding to a temperature of 21.1 K [7].

4. Heat transfer model

Considering steady state refrigeration of the vessel, no motion of the liquid hydrogen, as well as no ϕ-angular dependence of the boundary conditions and of the thermal properties of all employed materials, allows heat transfer behavior, in each of the vessel's regions, to be captured by the differential equation (Bird et al., page 318, [8]):

$$0 = \frac{1}{r^2}\frac{\partial}{\partial r}\left(r^2 \cdot q_r\right) + \frac{1}{r \cdot \sin\theta}\frac{\partial}{\partial \theta}\left(\sin\theta \cdot q_\theta\right) \quad (3)$$

where q_r and q_θ represent heat fluxes in the directions r and θ, respectively. In turn, q_r and q_θ are given by the expressions:

$$q_r = -k\frac{\partial T}{\partial r} \quad (4)$$

$$q_\theta = -k \frac{1}{r} \frac{\partial T}{\partial \theta} \tag{5}$$

where k represents the thermal conductivity of the material and T is temperature. After substitution of (4) and (5), equation (3) can be rewritten as:

$$0 = \frac{\partial}{\partial r}\left(r^2 \cdot \sin\theta \cdot k \cdot \frac{\partial T}{\partial r} \right) + \frac{\partial}{\partial \theta}\left(\sin\theta \cdot k \cdot \frac{\partial T}{\partial \theta} \right) \tag{6}$$

Due to the problem's symmetry about the θ = 0, π axis, we can consider only half of the domain in the plane r-θ, as shown in fig. 1b. The problem's boundary conditions are then as follows:

$$T(\theta = \theta_n) = T_o \quad \forall r \in [r_1, r_2] \tag{7}$$

$$T(r = r_1,\ r_2) = T_o \quad \forall \theta \in [\theta_n, \pi] \tag{8}$$

$$T(\theta = \theta_n) = T_s \quad \forall r \in [r_4, r_5] \tag{9}$$

$$T(r = r_4,\ r_5) = T_s \quad \forall \theta \in [\theta_n, \pi] \tag{10}$$

$$T(r = R) = T_e \quad \forall \theta \in [0,\ \pi] \tag{11}$$

$$\frac{\partial T}{\partial r}(r = 0) = 0 \quad \forall \theta \in (0,\ \pi) \tag{12}$$

$$\frac{\partial T}{\partial \theta}(\theta = 0) = 0 \quad \forall r \in [0, R] \tag{13}$$

$$\frac{\partial T}{\partial \theta}(\theta = \pi) = 0 \quad \forall r \in [0, r_1] \cup [r_2, r_4] \cup [r_5, R] \tag{14}$$

where T_e is the ambient temperature (T_e = 300 K), T_o is the low temperature imposed on the inner cold sector (at the inner cooled shield, T_o = 21 K), and T_s is the temperature imposed on the outer cold sector (at the outer cooled shield, T_s = 80 K).

Introducing the dimensionless variables:

$$r^* = \frac{r}{R} \qquad \theta^* = \frac{\theta}{\pi} \qquad T^* = \frac{T - T_o}{T_e - T_o}$$

equation (6) can be written as:

$$0=\frac{\partial}{\partial r^*}\left(r^{*2}\cdot\sin\left(\pi\cdot\theta^*\right)\cdot k\cdot\frac{\partial T^*}{\partial r^*}\right)+\frac{\partial}{\partial\theta^*}\left(\frac{\sin\left(\pi\cdot\theta^*\right)}{\pi^2}\cdot k\cdot\frac{\partial T^*}{\partial\theta^*}\right) \tag{15}$$

This equation is valid in the liquid hydrogen and each material of the insulated vessel as long as the proper value of thermal conductivity is used. Therefore we can write equation (15) for six different sub-domains (i=1,..6), obtaining a system of six differential equations, as indicated below:

$$0=\frac{\partial}{\partial r^*}\left(r^{*2}\cdot\sin\left(\pi\cdot\theta^*\right)\cdot k_i\cdot\frac{\partial T_i^*}{\partial r^*}\right)+\frac{\partial}{\partial\theta^*}\left(\frac{\sin\left(\pi\cdot\theta^*\right)}{\pi^2}\cdot k_i\cdot\frac{\partial T_i^*}{\partial\theta^*}\right)\quad \text{for i=1,..6} \tag{15-i}$$

where T_i^* is the dimensionless temperature in subdomain i and k_i is the thermal conductivity in subdomain i ($k_i = k_i(T_i^*)$). Thus equation (15-i) is valid for subdomain i. subdomain 1 (r^* є [0, $r_1^*=r_1/R$], θ^* є [0, 1]) is the liquid hydrogen; subdomain 2 (r^* є [r_1^*, $r_2^*=r_2/R$], θ^* є [0, $\theta_n^*= \theta_n/\pi$]) is the inner actively cooled shield (copper); subdomain 3 (r^* є [r_2^*, $r_3^*=r_3/R$], θ^* є [0, 1]) is the vessel wall (aluminum); subdomain 4 (r^* є [r_3^*, $r_4^*=r_4/R$], θ^* є [0, 1]) is the inner insulation layer; subdomain 5 (r^* є [r_4^*, $r_5^*=r_5/R$], θ^* є [0, θ_n^*]) is the outer actively cooled shield (copper); and subdomain 6 (r^* є [r_5^*, 1], θ^* є [0, 1]) is the outer insulation layer. k_1; k_2 and k_5; k_3; k_4 and k_6 are the thermal conductivities of hydrogen; copper; aluminum; thermal insulator respectively.

The resulting system of six second-order partial differential equations is solved for T_1^*, T_2^*, T_3^*, T_4^*, T_5^* and T_6^*, as functions of r^* and θ^*, when combined with 28 boundary conditions. In addition to the boundary conditions implied by (7) - (14) we must consider the continuity of the temperature ((26-i)) and the continuity of the radial heat flux ((27-i)) at the interface between two subdomains. Therefore the complete set of 28 boundary conditions is:

$$T_2^*(\theta^*=\theta_n^*)=0\quad \forall r^*\in\left[r_1^*,r_2^*\right] \tag{16}$$

$$T_1^*(r^*=r_1^*)=0\quad \forall\theta^*\in\left[\theta_n^*,1\right] \tag{17}$$

$$T_3^*(r^*=r_2^*)=0\quad \forall\theta^*\in\left[\theta_n^*,1\right] \tag{18}$$

$$T_5^*(\theta^*=\theta_n^*)=\frac{T_s-T_o}{T_e-T_o}\quad \forall r^*\in\left[r_4^*,r_5^*\right] \tag{19}$$

$$T_4^*(r^*=r_4^*)=\frac{T_s-T_o}{T_e-T_o}\quad \forall\theta^*\in\left[\theta_n^*,1\right] \tag{20}$$

$$T_6^*(r^*=r_5^*)=\frac{T_s-T_o}{T_e-T_o}\quad \forall\theta^*\in\left[\theta_n^*,1\right] \tag{21}$$

$$T_6^*(r^*=1)=1 \quad \forall \theta^* \in [0,1] \tag{22}$$

$$\frac{\partial T_1^*}{\partial r^*}(r^*=0)=0 \quad \forall \theta^* \in (0,1) \tag{23}$$

$$\frac{\partial T_i^*}{\partial \theta^*}(\theta^*=0)=0 \quad \forall r^* \in \text{ Subdomain } i \quad \mathit{for}\ i=1,..6 \tag{24-i}$$

$$\frac{\partial T_i^*}{\partial \theta^*}(\theta^*=1)=0 \quad \forall r^* \in \text{ Subdomain } i \quad \mathit{for}\ i=1,3,4,6 \tag{25-i}$$

$$T_i^*(r^*=r_i^*)=T_{i+1}{}^*(r^*=r_i^*) \quad \forall \theta^* \in \left[0,\theta_n{}^*\right] \ \mathit{for}\ i=1,..5\ ;\ \forall \theta^* \in \left[\theta_n{}^*,1\right] \ \mathit{for}\ i=3 \tag{26-i}$$

$$k_i \frac{\partial T_i^*}{\partial r^*}(r^*=r_i^*)=k_{i+1}\frac{\partial T_{i+1}{}^*}{\partial r^*}(r^*=r_i^*) \quad \forall \theta^* \in \left[0,\theta_n{}^*\right] \ \mathit{for}\ i=1,..5\ ;\ \forall \theta^* \in \left[\theta_n{}^*,1\right] \ \mathit{for}\ i=3 \tag{27-i}$$

5. Numerical solution

For effective storage of the hydrogen in the vessel, it is necessary to maintain the temperature of the liquid hydrogen low enough to keep it in the liquid phase. The temperature profile in the liquid hydrogen can be found by solving the system of equations (15-i)(i=1,..6) for a particular vessel configuration (specific values of r_i^*, R and θ_n^*). The vessel configuration considered here (see Table 1) possesses an external volume of 200 L, and can store up to 6.8 kg of liquid hydrogen at 21.1 K and saturation pressure of 0.1286 MPa. This amount of hydrogen provides a 483-805 km range for a mid-size class fuel cell powered automobile [3].

Table 1
Vessel configuration

Dimensionless values		Actual values (mm)		Layer thickness (mm)	
r_1^*	0.7865	r_1	285.5		
r_2^*	0.7879	r_2	286.0	Inner copper	0.5
r_3^*	0.7906	r_3	287.0	Aluminum	1.0
r_4^*	0.9063	r_4	329.0	Inner. therm. ins.	42.0
r_5^*	0.9077	r_5	329.5	Outer copper	0.5
		R	363.0	Outer. therm. ins.	33.5
θ_n^*	0.995	θ_n	179.1°		

The program FEMLAB® version 2.3b was used for the numerical calculation. With this software, the aforementioned PDE (Partial Differential Equation) problem is approximated using the Finite Element Method (FEM), [9]. FEMLAB® generates automatically a triangular mesh that covers the domain under consideration and takes into account the problem geometry. The solution presented in this paper was obtained using the adaptive mesh generation tool of FEMLAB®, which identifies the regions where high resolution is needed and produces an appropriate mesh, [9].

An approximate numerical solution, obtained with a mesh of 219,391 elements, is presented in Fig. 3. The temperature in the inner copper layer, the aluminum vessel wall, and the liquid hydrogen, was found to be below 21.11 K, as shown in Fig. 4. This simulation indicates that the highest temperature in the liquid hydrogen is attained at the interface with the inner copper layer ($r^* = r_1^* = 0.7865$) and at $\theta^* = 0$ (the furthest location from the inner cold sector). The calculated temperature at this point is $T\,(0.7865,\,0) = 21.106$ K. The numerical solution for the heat flux in the θ-angular direction is shown in Figs. 5 and 6, for sections next to the inner and outer cold sectors, respectively.

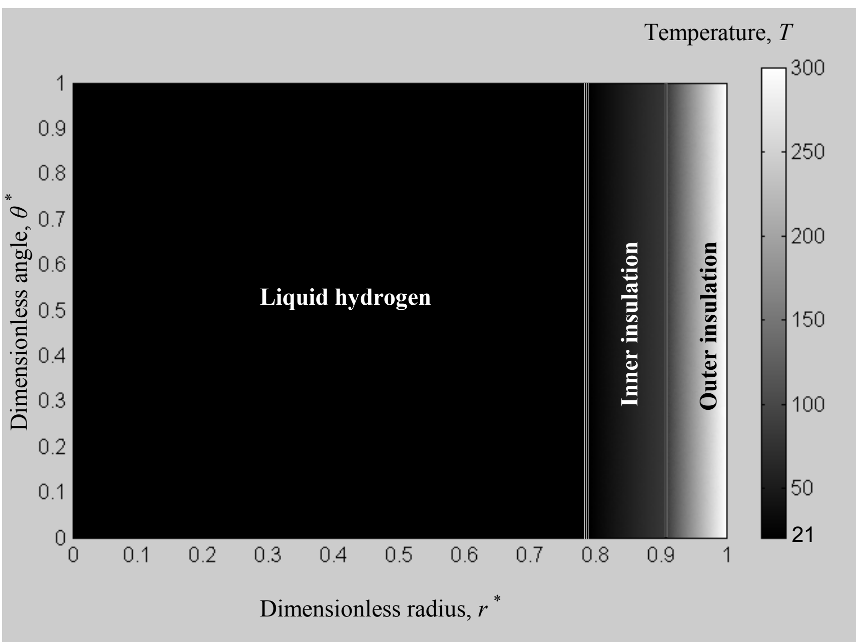

Fig 3. Temperature profile in the conduction-cooled liquid hydrogen storage vessel calculated with a mesh of 219,391 elements.

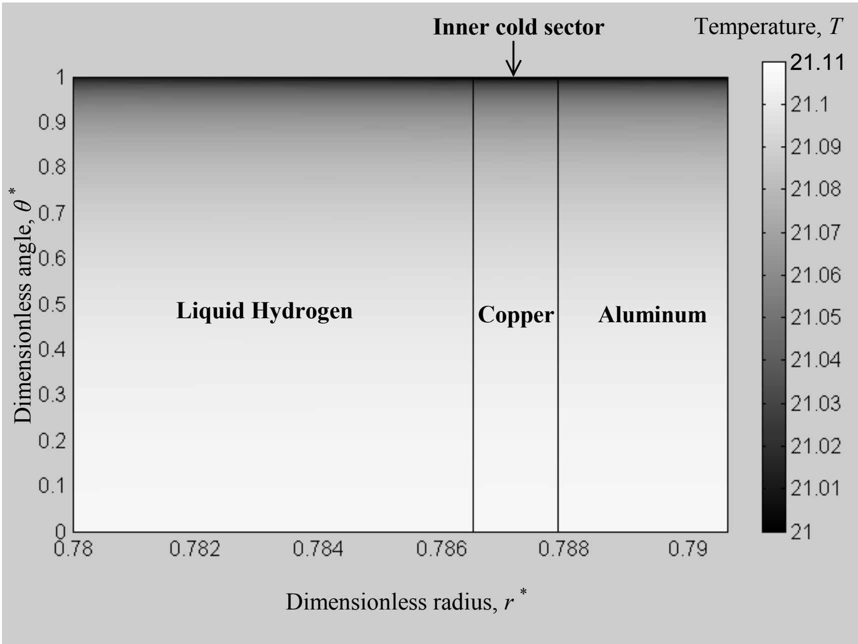

Fig 4. Temperature profile in the inner copper layer, the aluminum vessel wall and the section of the liquid hydrogen near the copper layer. The highest temperature in the liquid hydrogen is $T\,(0.7865,\,0) = 21.106$ K.

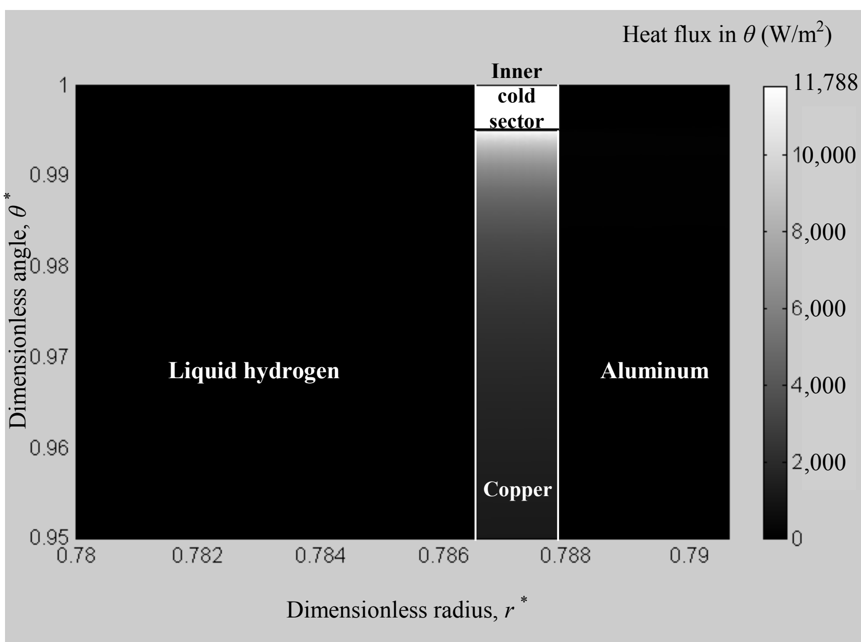

Fig 5. θ-angular heat flux profile in a section next to the inner cold sector in the conduction-cooled liquid hydrogen storage vessel.

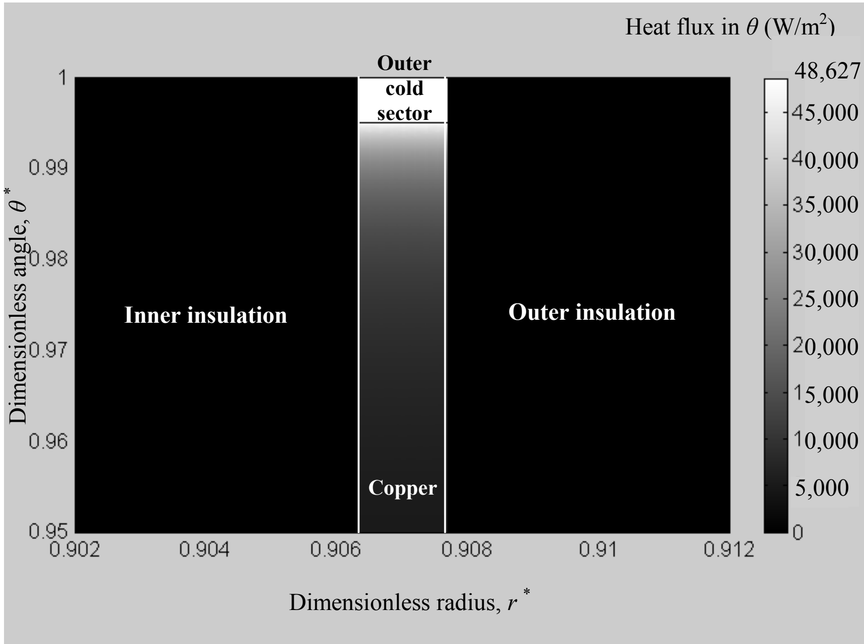

Fig 6. θ-angular heat flux profile in a section next to the outer cold sector of the conduction-cooled liquid hydrogen storage vessel.

6. Discussion

The studied vessel configuration allows the maintenance of the temperature in the liquid hydrogen close to the temperature in the inner cold sector (within less than 0.11 K difference), so hydrogen is maintained in the liquid phase for storage pressure of 0.1286 MPa and above.

From Fig. 5 it can be noted that the θ-angular heat flux is higher in the copper layer than in the other regions. In fact, it is about two orders of magnitude higher than the θ-angular heat flux in the aluminum wall and over four orders of magnitude higher than that in hydrogen. Similar calculation of the heat flux in the outer copper layer (Fig. 6) shows that the θ-angular heat flux in the outer copper layer is over six orders of magnitude higher than that in the thermal insulation layers. The copper layers are the preferred tracks for the heat, so that most of the heat that enters the vessel radially through the outer insulation layer, travels along the copper layers towards the cold sectors. As shown in Fig. 6, the heat flux increases significantly in the copper region, for θ^* above 0.95. Integration of the θ-angular heat flux over the boundary of copper at the outer cold sector (see Fig. 6), gives the θ-angular heat flow, and addition of the radial heat flows entering the cold sector through the thermal insulation layers, gives the total heat flow transferred to the outer cold sector. Integrating over the ϕ-angular direction yields an overall heat flow to the outer cold sector of about 0.948 W, with almost 80% of this heat exiting through the outer copper layer. Similarly, it is calculated that a heat flow of 0.180 W is transferred through the inner cold sector.

Removal of these heat loads at cryogenic temperatures (T_o = 21 K and T_s = 80 K) can be achieved using cryocoolers. The required cryocooler input power, P_c (W), and the estimated cryocooler mass, M_c (kg), can be approximated as functions of the temperature and the cooling load Q_c (W), as indicated below, [10,11]:

$$P_c = 3.966 + 14.58 \cdot Q_c + 0.0038376 \cdot Q_c^{\,2} \quad \text{at 80 K} \tag{28}$$

$$P_c = 100.98 + 151.18 \cdot Q_c + 0.87815 \cdot Q_c^{\,2} \quad \text{at 21 K} \tag{29}$$

$$M_c = 157 \cdot \exp(-0.0533 \cdot T) \cdot Q_c^{\,0.009 \cdot T + 0.1275} \tag{30}$$

Application of these relations to the cooling loads required by the liquid hydrogen vessel studied in this section, that employs two actively cooled copper shields, results in the need of two cryocoolers with the following characteristics: one 29.79-kg cryocooler with input power of 128.206 W necessary to remove 0.180 W at 21 K from the inner copper layer (corresponding to a refrigerator's Carnot efficiency of 1.86 %); and one 2.11-kg cryocooler with input power of 17.797 W necessary to remove 0.948 W at 80 K from the outer copper layer (Carnot efficiency is 14.65%).

If it is considered that the vehicle's hydrogen fuel cell is used for generation of the power required for active cooling of the liquid hydrogen vessel, a hydrogen consumption rate of 12.05 g/h would be necessary to generate the required 146.003 W (assuming fuel cell conversion of 12.117 W-h/gH_2 estimated for Ballard's Nexa® power module), and the vehicle would run out of hydrogen in 23.5 days, if parked after complete filling of the vessel with liquid hydrogen at 21.1 K and pressure of 0.1286 MPa or slightly higher.

Let us consider a situation where the vehicle is parked and the power provided to the 21 K-cryocooler is less than the estimated requirement of 128.206 W. Since the cryocooler's cooling capacity will be lower than 0.180 W, this will result in heat flow into the liquid hydrogen with consequent temperature increase up to saturation, followed by hydrogen evaporation, and over-pressure if hydrogen is not removed from the vessel at the same (or higher) rate with which it evaporates. It would be possible to achieve operation at constant temperature and pressure (saturation) inside the vessel if hydrogen gas is removed from the vessel at the same rate of evaporation, and with lower power consumption in the 21 K-cryocooler than the requirement calculated for zero hydrogen boil-off. Furthermore, hydrogen gas removed from the vessel could be used in the vehicle's fuel cell for generation of power that is made available to run the cryocoolers.

If the 21 K-cryocooler were shutdown, it would still be possible to maintain approximate temperature of 21.1 K and (saturation) pressure of 0.1286 MPa inside the vessel, as long as hydrogen can evaporate at a rate of 1.60 g/h (vaporization rate resulting from a heat flow of 0.180 W, given a hydrogen vaporization latent heat of 404.35 J/g, [7]) and exit the vessel at the same rate. Fuel cell power generation with this amount of hydrogen results in 19.407 W, just above the power required to run the 80 K-cryocooler (17.797 W). In this case, the vehicle would run out of hydrogen in 177 days, if parked after complete filling of the vessel with liquid hydrogen at 21.1 K and saturation pressure of 0.1286 MPa. Besides much longer hydrogen availability, in this case it is necessary to provide the vehicle only with the 80 K-cryocooler, avoiding the heavier and less efficient 21 K-cryocooler.

7. Cryogenic compressed hydrogen gas storage

Similar calculations have been done for hydrogen gas storage at 80.6 K and 34.4 MPa, considering a conduction-cooled vessel with only one (inner) copper shield in contact with the hydrogen. The cold sector in this copper shield is kept at 80 K with the use of a cryocooler. No outer copper shield has been considered in this case. Vessel external volume is also fixed at approximately 200 L and hydrogen storage capacity set at 6.8 kg, for comparison with liquid storage. An insulated aluminum lined-fiber wrapped pressure vessel with performance factor of 1.3×10^6 inches, [3], is considered for hydrogen gas storage, since this type of vessel has already been tested at cryogenic temperatures [12]. The results for both compressed gas and low-pressure saturated liquid storage are summarized in Table 2. For the vessel configuration considered here, compressed gas storage at 80.6 K offers longer storage time before hydrogen depletion due to a lower in-leak heat, that also results in the need for a smaller cryocooler.

Table 2. Comparative results for active storage of cryogenic compressed hydrogen gas and saturated liquid hydrogen

Initial hydrogen phase	Gas	Saturated liquid
Stable hydrogen phase	Gas	Vapor-liquid equilibrium
Temperature (K)	80.6	21.1
Pressure (MPa)	34.4	0.1286
Internal volume (L)	109.7	97.5
External volume (L)	200.4	200.4
Hydrogen mass (kg)	6.8	6.8
Vessel wall material	Aluminum-lined, carbon fiber-wrapped	Aluminum
Inner copper layer thickness (mm)	0.5	0.5
Vessel wall thickness (mm)	11.5	1
Inner insulation thickness (mm)	N.A.	42
Outer copper layer thickness (mm)	N.A.	0.5
Outer insulation thickness (mm)	54	33.5
Temperature inner cold sector (K)	80	N.A.
Temperature outer cold sector (K)	N.A.	80
Total in-leak heat (W)	0.574	1.128
Cryocooler temperature (K)	80	80
Cryocooler cooling load (W)	0.574	0.948
Cryocooler Mass (kg)	1.38	2.11
Cryocooler input power (W)	12.329	17.797
Hydrogen required for power generation (g/h)	1.02	1.47
Hydrogen evaporation rate (g/h)	N.A.	1.60
Hydrogen loss (g/h)	1.02	1.60
Maximum storage time (days)	279	177

8. Conclusions

A liquid hydrogen storage vessel is proposed, that incorporates two copper layers in its thermal insulation. This storage vessel design directs the vessel's in-leak heat towards two cold sectors where cryogenic refrigeration is used to maintain the stored hydrogen in the liquid phase. Although evaporative loss of hydrogen is prevented with the proposed design, refrigeration work must be provided to remove the in-leak heat. Allowing hydrogen evaporation to produce hydrogen gas that can be used for power generation in the vehicle's fuel cell helps reduce the cooling load of the refrigerator(s). Application of the proposed conduction-cooling concept to the storage of cryogenic compressed hydrogen gas is also shown to be attractive. Finally, it is worth noting that a simple configuration of the vessel was used in this work to demonstrate the proposed concept. Research is currently underway to optimize this vessel configuration.

Acknowledgement

The authors gratefully acknowledge the financial support of the National Science Foundation under Grant CTS 0301931.

References

[1] Aceves SM, Berry GD, Rambach GD. Insulated pressure vessels for hydrogen storage on vehicles. Int. J. Hydrogen Energy, 1998;23(7):583-591.

[2] Berry GD, Aceves SM. Onboard storage alternatives for hydrogen vehicles. Energy & Fuels, 1998;12:49-55.

[3] James BD, Baum GN, Lomax FD, Thomas CE, Kuhn IF. Comparison of onboard hydrogen storage for fuel cell vehicles. Directed Technologies Report DE-AC02-94CE50389, prepared for Ford Motor Company, 1996.

[4] Manousiouthakis V, Kim YI, Posada A. Conduction-cooling of a superconducting cable. World Patent WO2005020245, 2005.

[5] Marquardt ED, Le JP, Radebaugh R. Cryogenic material properties database. Presented at the 11th International Cryocooler Conference, June 2000, Keyston, CO, USA.

[6] Simon NJ, Drexler ES, Reed RP. Properties of copper and copper alloys at cryogenic temperatures. National Institute of Standards and Technology. NIST Monograph 177, 1992.

[7] Lemmon EW, Peskin AP, McLinden MO, Friend DG. NIST 12, Thermodynamic and Transport Properties of Pure Fluids, NIST Standard Reference Database 12, Version 5.0, 2000.

[8] Bird RB, Stewart WE, Lightfoot EN. Transport Phenomena. New York: John Wiley & Sons, Inc, 1960.

[9] COMSOL AB. FEMLAB® Reference Manual. 2nd printing. Stockholm: COMSOL AB, 2001.

[10] Haberbusch MS, Stochl RJ, Culler A.J. Thermally optimized zero boil-off densified cryogen storage system for space. Cryogenics, 2004;44:485-491.

[11] Ter Brake HJM, Wiegerinck GFM. Low-power cryocooler survey. Cryogenics, 2002;42:705-718.

[12] Aceves SM, Martinez-Frias J, Espinosa-Loza F. Performance evaluation tests of insulated pressure vessels for vehicular hydrogen storage. Proceedings of the World Hydrogen Energy Conference, Montreal, Canada, June 2002.